About the problem of properly designed FE-Models for mechanical contact problems on layered materials

M. Herrmann(a), F. Richter(a), N. Schwarzer(b)

a) Solid State Physics, Institute of Physics, Chemnitz University of Technology, 09107 Chemnitz, Germany

b) Saxonian Institute of Surface Mechanics, Am Lauchberg 2, 04838 Eilenburg, Germany

Abstract

In this paper, limiting factors for contact modelling of layered materials using finite element (FE) solutions are presented. One has to note that a fundamental problem is attributed to the normal and lateral limitedness of the finite element model. The underlying parameters which influence the finite element results of the elastic stress field are identified based on comparison to a complete analytical solution for layered materials. With this in mind, homogeneous substrates and layered systems have been studied having different elastic moduli. Secondly, the influence of the normal and lateral dimensions of the finite element model on the contact solution is discussed. It was found that the deviation of the finite element contact force from that of the analytical solution is up to 10 % for homogeneous substrates. It is independent of the elastic modulus while the model size is the determining influence. These deviations are enhanced or extenuated by changing the indenter radius and model size, respectively. For layered systems, the ratio of Young's moduli of film/substrate and the contact radius to film thickness ratio are determining factors. The behaviour due to the geometrical limitedness of the FE model for the layered case is given in form of a rule of thumb. Additionally, for a stiff layer on compliant substrate a plate-like bending of the layer comes into play as another effect which is closely connected with the lateral size of the FE models.

1. Motivation

Since the last two decades, finite element calculations are frequently used as an established and trusted method for mechanical contact analyses [1-6]. Several commercial contact models are available. Based on the weak formulation, FE modelling is attached to finite domains and therewith is geometrically limited. This leads on the one hand to a necessary reduction of the CPU time by a properly chosen mesh size. On the other hand, a decrease of the model size results in a systematic distortion of the results, due to the boundaries. Typically deviations of up to 10 % are possible which affect - among others - the load depth curves. One should note that using FE modelling to fit e.g. Young's moduli can then lead to inaccuracies of about 10 % or more, depending on experimental data, used indenters, and so forth.
Considering their dimensions, typical samples (e.g. wafers having a thickness of several hundreds of μm) should be rather considered as homogeneous or layered halfspace than as FE domain. In the literature [1,3,6,8,9,12,18] upper ratios of contact radius to model dimension up to 0.05 are used. Often calculations are performed up to a ratio of final indentation depth to model dimension of about 0.01 to 0.3 depending on the type of the indenter**.** This raises the question for properly sized FE domains in order to keep the influence of the boundaries low.

In this work, we have investigated the influence of the dimensions of the FE model on the results for standard tasks of contact mechanics. An analytical method based on the extended Hertzian approach [15,19] which considers a layered halfspace was used for comparison.
First, a homogeneous body was investigated with varying FE model sizes, Young's moduli and indenter radii. In a second step, certain modulus combinations are studied as examples for the layered case. Finally, the results are discussed which show that FE modelling needs a problem-oriented choice of the model size depending on the contact situations.

2. Modelling mechanical contact

2.1 Analytical model

For the analytical modelling, the method of image loads (ILM) [13] was used. The ILM represents the generalisation of the indentation of a sphere into an infinite homogeneous halfspace (so called Hertzian indentation [14]) to the indentation into an infinite halfspace which is covered with one or more films having different elastic properties. The model allows the analytical evaluation of the complete elastic deformation and stress field within the film(s) and the substrate. It enables to simulate the elastic spherical indentation experiment, e.g. to calculate the load-displacement curve of the indenter for a given set of elastic properties. The ILM is based on the assumption that the contact stress has the well known Hertzian pressure distribution. For layered materials the contact stress distribution can differ significantly from the Hertzian one. In such cases, the extended Hertzian approach developed by one of the current authors [15,19] provides an adequate description. It allows dealing with surface stress distributions of the type

$$\sigma_{zz0}(r,\varphi) = \sum_{n=0}^{N} c_{\sigma n} r^n \sqrt{a^2 - r^2} \ . \tag{1}$$

In this approach, the generalised contact equation of the form

$$w_S(r) + w_I(r) = h - \frac{r^2}{d_0} - \frac{r^4}{d_2} - \frac{r^6}{d_4} - \frac{r^8}{d_6} \tag{2}$$

is valid. Here, w_I and w_S are normal surface displacement of indenter and sample body, respectively, h is the indentation depth, r the distance to the contact centre, and the d_i (i = 0, 2, 4, 6) are parameters depending on the shape of both indenter and sample-body. This approach opens up a wide range of modelling mechanical contact for indenters having symmetry of revolution [16]. The necessary evaluations had been performed by means of a specific software package [17].

2.2 Finite Element Model

Spherical indentation was modelled assuming a rigid indenter with varying radii in the range of 2.5 µm to 200 µm. The rigid indenter was chosen in order to avoid inaccuracies due to the two body contact. This specification does not affect the generality of the conclusions drawn at the end of this paper. An axisymmetric formulation of the contact problem was used in ANSYS. Maximum indentation depth was chosen as length parameter of the model and set at 0.9 µm. The film thickness was given the same value. The model sizes in r- and z-direction were chosen to be larger than the said 0.9 µm by a size factor x equal to 50, 100, 200, 500, 1000, and 1500.
A symmetry boundary condition was set at the centre line and no displacement at bottom surface was allowed. The outside of the specimen was free. Linear elastic behaviour with

Young's moduli and Poisson ratio was used as constitutive equation. The elastic material parameters were oriented on real mechanical properties (see Table I) to cover the whole region of interest.
For both FE and analytical modelling no friction at the indenter-sample boundary was considered, i.e. both bodies could move freely in lateral direction at the boundary.
The FE calculation was performed using a displacement control up to the final penetration depth of abovementioned 0.9 µm. After the indenter has reached the displacement this value, the reaction forces detected at bottom surface have been summed up to get the corresponding contact force. This sum has been checked with the sum of the nodal forces of the contact elements which should be equal, thus allowing to monitor a less accurate calculation.
To perform the comparison of FE and analytical model, two approaches have been used in order to understand the mechanical contact in detail. The first way was to compare the contact forces necessary to achieve 0.9 µm final penetration depth. Also the resulting contact stress distribution and the von Mises stress along the axis of symmetry have been investigated. In a second approach, the FE bottom boundary condition of zero displacement was simulated in our analytical model by considering a layer with a thickness equal to FE model size in z-direction on a nearly infinitely stiff substrate. This model, which considers the limitedness of the FE model with respect to the vertical but not the lateral direction is referred to in the following as "vertically limited analytical model".

Table I. Overview of the input material parameters

	Corresponding. Material	**Young's modulus [GPa]**	**Poisson ratio**
Sample 1100	diamond	1100	0.07
Sample 420	sapphire	420	0.234
Sample 210	steel	210	0.3
Sample 72	fused silica	72	0.17
Sample 50	amorphous SiC:H	50	0.25
Sample 30	amorphous SiC:H	30	0.25
Sample 4	low-k dielectrics	4	0.25

3. Results

In the first part we have analysed the contact of an indenter and a homogeneous sample. Then we extended our study to a single layer on a substrate.

3.1 Homogeneous sample

In a first step, sphere radius and penetration depth were kept constant and the model size was increased. Therewith, the ratio of final indentation depth to model size, h/x, is not constant. Secondly, the indenter radius was varied while the penetration depth and the model size remained constant. For this is given, that the ratios of contact radius to indenter radius, a/R, or final indentation depth to indenter radius, h/R, were varied.

3.1.1 Constant radius and indentation depth, increase of the model size

The deviation of the contact force determined by FEM from that calculated using the analytical model (referred to in the following as "analytical force") is plotted in Fig. 1. The results for one material as example namely S 210 are shown in Table II. The analytical force, FE contact force (both for 0.9 µm indentation depth) as well as their relative difference for sample 210 are given with increasing model size. The deviation decreases from 10.3 % down

to 1.4 % for the largest model. For all materials the contact force for the FE model is always bigger than that calculated with the analytical model (Fig. 1). This is plausible since due to the limitedness of the considered volume in the FE model the material has a larger resistance against the indentation. It follows that the deviation of the contact forces is 10.3 % for the smallest FE models (x = 50) and goes down to 1.4 % for the largest models.
There is no clear influence of the material as the sequence of the materials with respect to the deviation is not constant from one model size to the other.

Table II. Analytical force together with FE-forces and relative deviation for different model dimensions (indentation depth 0.9 µm, indenter radius 20 µm)

	Model	Analytical force, F_a [N]	FE-force, F_{FE} [N]	$\Delta F/F_a$
Sample 210	1:50	1.17	1.290	0.1030
	1:100	1.17	1.231	0.0520
	1:200	1.17	1.214	0.0376
	1:500	1.17	1.212	0.0360
	1:1000	1.17	1.208	0.0327
	1:1500	1.17	1.187	0.0141

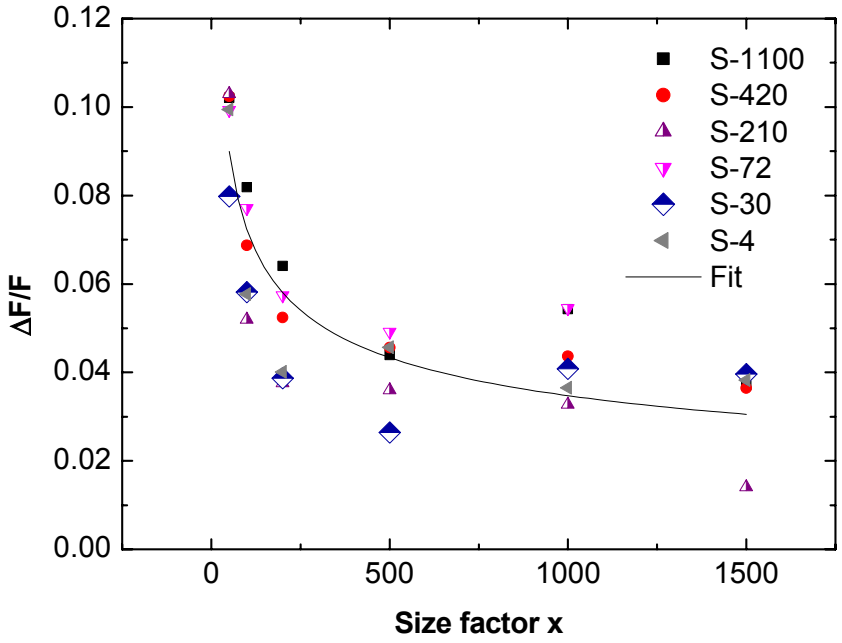

Figure 1. Relative deviations of the FE-contact forces from the analytical force as a function of the model size for different materials.

It seems that a function like $y = C \cdot x^n$ is a plausible description of the occurring influence. It converges to zero for large x and it increases for smaller models. As fit results a constant C = 0.316 and a value of n = -0.319 were found. However, for smaller models it will lose its sense and the whole regime tends to be dominated by a plate-like bending of the substrate.
Additionally, we have examined the contact stress distributions calculated by both the FE and the analytical model. The resulting distributions for sample 210 (x = 100 for the FE model used) are shown in Fig 2. The contact radii are 4.19 µm for the analytical and 4.35 µm for the FE model.

In addition, a vertically limited analytical model was used to simulate the FE model of size factor x. For that purpose, the vertical FE size was used as film thickness on a nearly infinitely stiff substrate to enforce no displacement in z-direction. The obtained contact stress is also plotted in Fig. 2 and the contact radius results in a value of 4.27 µm. The curve shape of the contact stress for the vertically limited analytical model lies in between the shapes of FE and analytical model. The curve shape is nearly the same in the centre of contact for FE and vertically limited analytical model. The curve shape of the vertically limited model follows the analytical one more closely in outward direction. Therewith, the behaviour of the contact stresses of all three models is plausible. The FE boundary at the bottom leads to an increased contact stress in the centre of the contact. The better agreement to the analytical one in the lateral direction also shows the influence due to the bottom boundary.
As another measure for comparison we have used the maximum of the contact pressure distribution (i.e. the contact pressure in the centre of contact) at maximum load, which consequently shows the same behaviour as the contact forces. The obtained values are plotted in Fig. 3. In agreement with the special case shown in Fig. 2, the stress values for the FE model are larger than those calculated with the analytical model which is in accordance with the expectations as discussed with Fig. 1. The relative deviation for all materials is less than 3 % and goes down with larger model dimensions.
The maximum of the von Mises stress distribution (not shown) has the same behaviour, i.e., it is larger for the FE model than for the analytical model, and this difference goes down with increasing FE model size. The deviation is in the range from 1 % to 3 % and is discussed later.

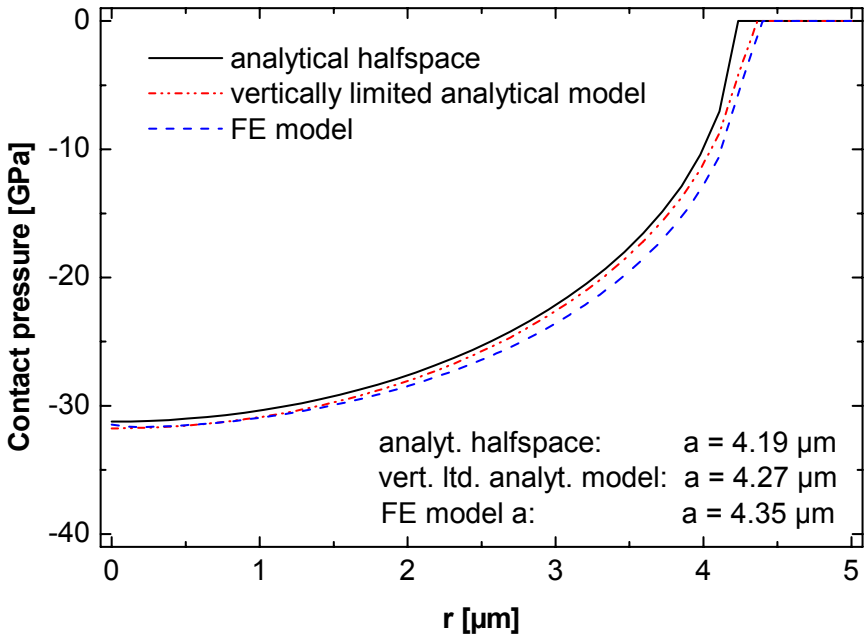

Figure 2. Comparison of the contact stress distribution at maximum load for sample S210 obtained by i) the analytical halfspace model (solid line), ii) vertically limited analytical model simulating the x = 100 FE model (dash dotted line), and iii) the x = 100 FE model (dashed line). Additionally, the resulting contact radii are given.

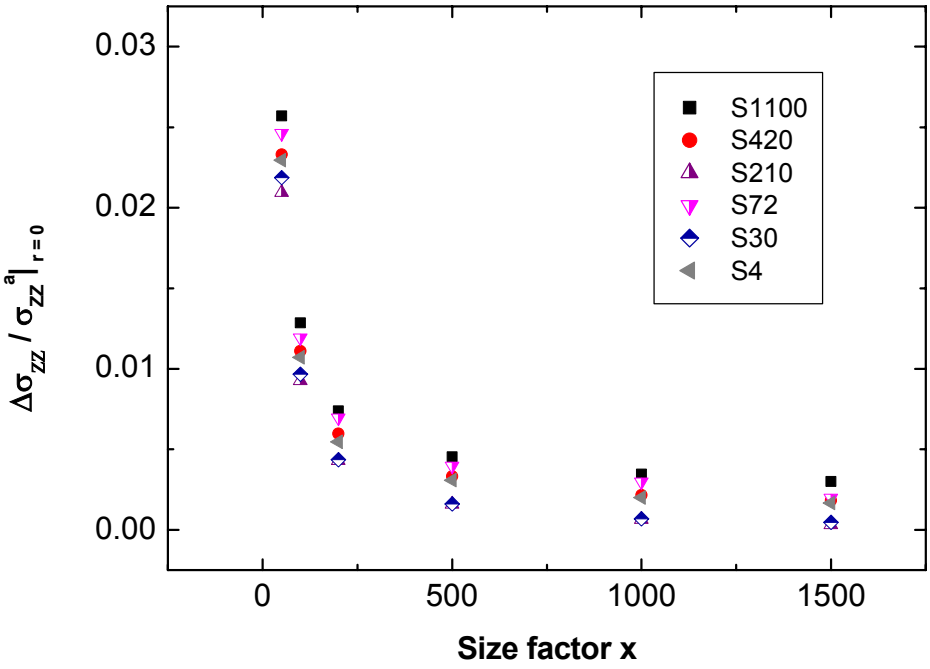

Figure 3. Relative deviations of the contact stress maxima as a function of the FE model size for all materials.

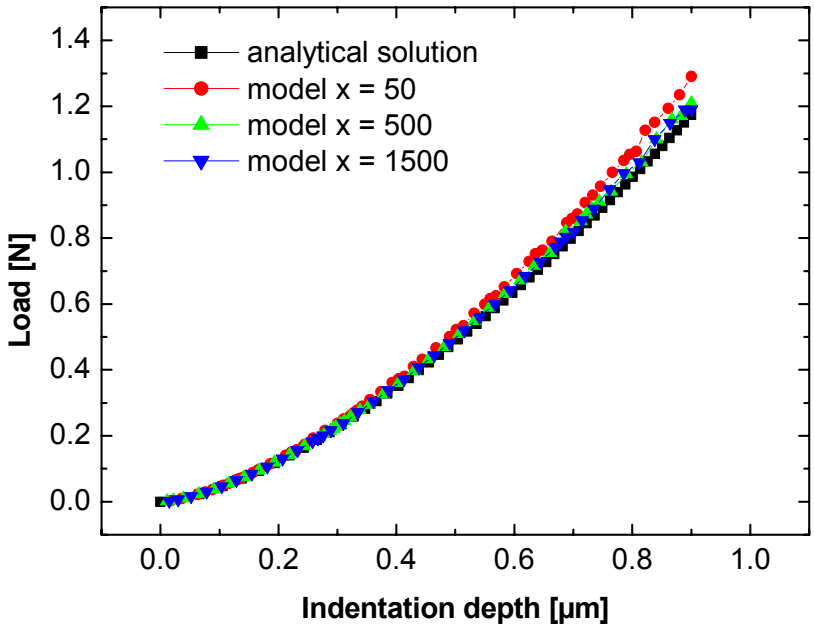

Figure 4. Load depth curves for spherical indentation with radius of 20 µm in S 210 which shows the influence of the FE size parameter x compared to the analytical solution. The deviation to the analytical model decreases with increasing model size.

Another important output of the calculations is represented by the elastic load depth curves which can be used to derive Young's modulus or other parameters (stress-strain curve). The

load depth curves for spherical indentation of 20 µm calculated by the analytical as well as different FE models (x = 50, 500 and 1500, resp.) are plotted in Fig. 4. It can clearly be seen that the smaller FE models yield a higher force for the same displacement. Increasing the model matches the curve obtained from the analytical model much better. A final deviation of 1.4 % remains for the x = 1500 model in case of S210 (cf. Table I).

3.1.2 Constant model size and indentation depth, increase of the indenter radius

In the following, the final displacement was held constant and the indenter radius was varied between 2.5 µm and 200 µm. The ratio of contact radius to indenter radius, a/R, decreases from 0.6 to 0.07 with increasing radius R. The contact forces at the maximum displacement 0.9 µm received by FE and analytical modelling as well as their relative difference are given in Table III. The relative deviations of the maxima of the contact stress distributions are also listed in Table III.
The resulting dependencies of the deviations on the model size (rightmost two columns) are visualised in Fig. 5. Both parameters decrease with increasing indenter radius. The deviation of the force goes down from 8.6 % to a nearly constant level of about 1-1.5 %, and for the contact pressure it drops from about 3 % to 0.4 %. The drop is significantly from 2.5 µm to 20 µm of radius and then it slightly increases or is nearly constant.

Table III.
Contact force at maximum displacement received by FE (x = 1500) and analytical model together with their relative difference as well as the analogue relative difference of the maximum contact pressures as a function of indenter radius.

	Indenter radius [µm]	**Analytical force, F_a [N]**	**FE-force, F_{FE} [N]**	**$\Delta F/F_a$**	**$\Delta\sigma_{ZZ}/\Delta\sigma_{ZZ}^a\vert_{r=0}$**
Sample 210	2.5	0.402	0.437	0.08570	0.0290
	5	0.578	0.612	0.05866	0.0167
	10	0.824	0.856	0.03824	0.0103
	20	1.170	1.187	0.01410	0.0003
	100	2.627	2.658	0.01184	0.0042
	200	3.715	3.776	0.01634	0.0042

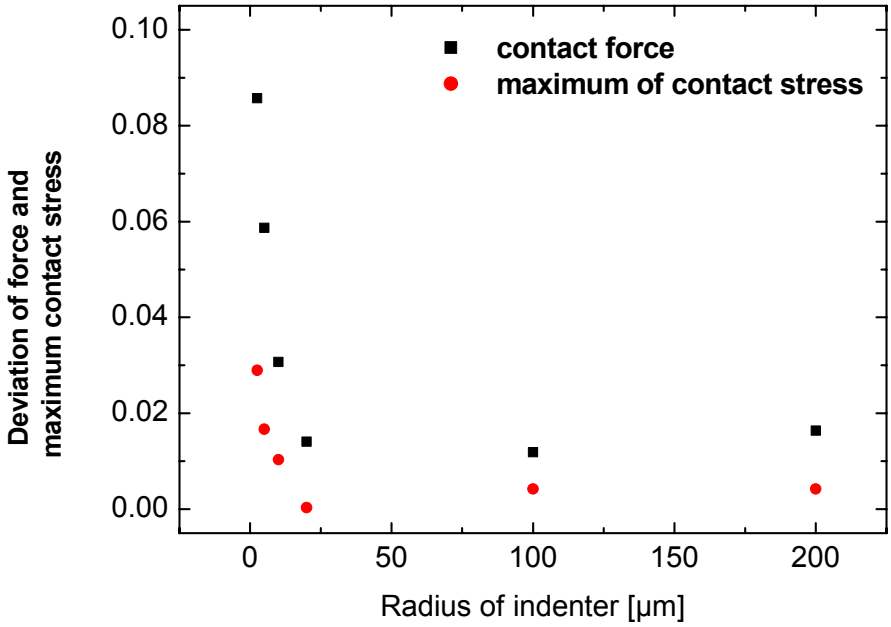

Figure 5. FE (x = 1500 model) vs. analytical modelling results: relative deviations of contact force and maximum contact pressure at maximum indentation depth of 0.9 µm in dependence on the indenter radius.

3.2 Single layer at a substrate

Three single layer-substrate systems were studied: a stiff film of S 210 on substrates of S 50 and S 4, resp., as well as a compliant S 50 layer on a stiff S 210 substrate. The film thickness was set equal to the abovementioned length parameter of 0.9 µm. FE models of x = 100 and x = 1500 were chosen.

The investigated cases and the resulting forces are listed in Table IV. In case of a stiffer film on a less stiff substrate, the FE forces overestimate the contact force by about 4 % for S 210 on S 50 and by 1 % for the S 4 substrate. This is the same trend of overestimation as for a less stiff film on a stiffer substrate, where the deviation is about 9 %. Increasing the model size leads to a reduction of the overestimation.

Remarkable is the fact that for S 210 on S 4 in case of the larger FE system (x = 1500) a contact force smaller than that of the analytical model was received. This is discussed below.

The contact stress distributions for the analytical solution compared to the FE solution are plotted in Fig. 6. For stiff films on less stiff substrates one finds a large difference to the well known Hertzian contact stress distribution, which in fact is not surprising: the Hertzian contact pressure distribution was derived for a homogeneous halfspace which is not considered here. In addition, it is known [19] that a large difference in Young's modulus between film and substrate causes particularly large deviation from the Hertzian case. It is also shown in Fig. 6 that the contact radii of the FE solution are larger than those determined by the analytical model.

Table IV.
Analytical force together with FE-forces and relative deviation for different model dimensions and layer-substrate combinations

Film on substrate	Indenter radius [µm]	Analytical force, F_a [mN]	FE model size factor x	FE-force, F_{FE} [N]	$\Delta F/F_a$
S 210 on S 50	20	31.05	100	32.33	0.0412
			1500	31.52	0.0151
S 210 on S 4	20	29.85	100	30.16	0.0104
			1500	29.29	-0.0188
S 50 on S 210	20	875.0	100	951.6	0.0875
			1500	911.9	0.0422

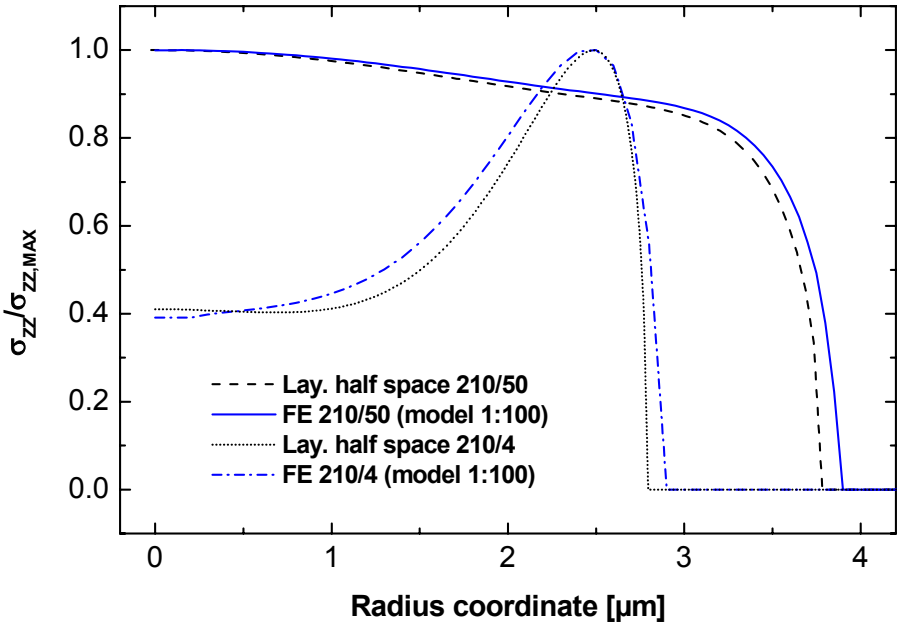

Figure 6. Contact stress distributions of S 210 on S 50 and S 210 on S 4 for the analytical halfspace solution compared to the FE model (x=100).

4. Discussion

4.1 Homogeneous sample

In order to understand our results better we have used the vertically limited analytical model in addition to the analytical halfspace model and different FE models characterised by their size factor x. We will discuss this using the homogeneous sample S210 as an example (cf. Fig. 2). The first observation is the smaller contact radius of the halfspace solution compared to the other cases which are relatively close together. Secondly, we found that the maximum of the contact stresses of the FE model and the vertically limited analytical model are nearly equal. This shows that the limitedness of the FE models leads to an increased contact pressure, and therewith contact force in comparison to the analytical model. This is plausible because to achieve the same final displacement with the FE model a higher force is necessary

because of the smaller volume of deformable material within the FE boundaries. For the x = 100 model the contact force necessary to reach a displacement of 0.9 µm is 1.23 N compared to 1.17 N for the analytical solution. The vertically limited analytical model which simulates the stiff FE bottom boundary needs an increased contact force of about 1.21 N. It should be mentioned that the simulated FE model lies between the real FE model and the analytical model, and helps to understand the regime.
An increased maximum of the von Mises stress is induced by including the bottom boundary in the analytical model. Increasing the FE model size will also result in smaller maxima of von Mises stress, which we have found.
To demonstrate the extent of the deformation field we calculated the normal deformation which is obtained in a depth where the deformation is forced to zero by the FE model boundary. The resulting deformation in a depth comparable to the FE model of x = 100 is around 0.03 µm or normalised to the final penetration depth to 3.3 %. This means in reality one would find a deformation of 0.03 µm, but the FE domain brings the occurring deformation to zero. For model size x = 1500 the normal deformation at the bottom boundary is about 0.5 nm or 0.06 %, respectively. We conclude that the deformation at the bottom side should be nearly zero to minimize the influence of the finite FE domain on the results.
For this part of the study, the ratio of penetration depth to indenter radius was held constant at 0.9 µm and only the varying model size causes the deviation between FE and analytical modelling.
From the load depth curves (Fig. 4) we see that the deviation becomes larger with increasing penetration depth or contact radius at a constant indenter radius and model size.
The dependence of the deviation on the indenter radius at the given constant maximum indentation depth of 0.9 µm is attributed to a varying ratio of indentation depth to contact radius or contact radius to indenter radius. The ratio of contact radius to sphere radius decreases from about 0.6 to 0.07 by increasing the radius from 2.5 µm to 200 µm and is combined with decreasing deviation.
In contrast to [8] where an allowed contact to indenter radius ratio, a/R, of 0.5 is recommended our results suggest a smaller a/R of about 0.2 to be maintained.
Remembering that the model size and the final indentation depth are constant and only the indenter radius was varied the key parameter is the ratio of contact radius to indenter radius, a/R, which is proportional to the indentation strain for spherical loading.

4.2 Single layer

Both combinations of a film and substrate, i.e. stiffer film on less stiff substrate and vice versa, show a larger FE contact force than the force for the analytical layered halfspace model. Furthermore, a larger model size decreases the deviation. It seems that the finite domain size of the FE model is one of the determining factors.
Similar to the investigations presented in this paper we have performed a systematic comparison of the results of FE and analytical modelling for bulk and layered samples. In the analytical models we considered vertical limitedness as shown above as well as lateral limitedness using a method described in [20,21]. These investigations showed that the distortion of FE results due to the geometrical limitedness of the model is greatly increased for layered samples in comparison to homogeneous ones. The extent of deviation depends on the ratio of Young's moduli of film and substrate as well as on the size of the volume essentially involved in the interaction in comparison to the film thickness. For the latter, the ratio a/t (a - contact radius, t - film thickness) was found to be a proper description.

If the distortion of FE results found in case of a homogeneous sample shall be maintained when a layered sample is to be treated, the size of the FE model has to be increased. We found - as a rule of thumb - the following formula to be valid:

$$X_{layered} = X_{\mathrm{hom}og.} \cdot \frac{E_{\max}}{E_{\min}} \cdot \begin{cases} 1 & \forall\ a \le t \\ a/t & \forall\ a > t. \end{cases} \qquad (3)$$

Here, $X_{layered}$ and $X_{homog.}$ are the size of the FE model in the layered and homogeneous case, and E_{max} and E_{min} are the larger and the smaller of the moduli of layer and substrate, respectively.
The negative deviation observed in one case (cf. Table IV) is reasonable if one considers the situation as a plate-like bending of the stiff layer. The outside boundary in r-direction of the FE model is free. Therewith, the stiff layer can easier follow the deformation in z-direction because the other end of the film at the outer boundary is not fixed. This influence is more pronounced for smaller FE models, and is superimposed by the effect due to the bottom FE boundary.

5. Conclusion

Based on comparison with an analytical model it was found that FE modelling results shows systematic deviations of up to 10 % due to their geometrical limitedness in r- and z-direction. Homogeneous and single layer samples have been studied. Determining parameters for the homogeneous case are the ratios of penetration depth or contact radius to model size (h/x or a/x) as well as contact radius to indenter radius (a/R) depending on the specific contact situation.
The calculations have shown that the model size has to be at least 1000 times the indentation depth in order to get a sufficiently small influence due to limitedness of the FE model.
Secondly, the ratio of contact radius to indenter radius should be less than 0.2 for a given model size.
For the layered case a rule of thumb (cf. Equation 3) was given in order to consider the additional influence of the FE model size with respect to the homogeneous case. The ratio of Young's moduli for film and substrate and the ratio of contact radius to film thickness were identified as determining parameters. The larger the ratios of the moduli and contact radius to film thickness are, the larger the FE model size has to be. As an example, considering a Young's moduli ratio of 4 and a ratio of contact radius to film thickness of about 4 would lead to a necessary increase of the FE model size by a factor of 16.
Finally, this study should help to improve the accuracy of FE calculations for applications, e.g. indentation of layer-substrate compounds in microelectronics or for hard coatings, which in reality should be rather considered as layered homogeneous halfspace.

6. References

[1] T.Y. Tsui, J. Vlassak, W.D. Nix, J. Mater. Res. 14 (1999) 2196-2203.
[2] T.Y. Tsui, J. Vlassak, W.D. Nix, J. Mater. Res. 14 (1999) 2204-2209.
[3] A. Bolshakov, G.M. Pharr, J. Mater. Res. 13 (1998) 1049-1058.
[4] G. Carè, A.C. Fischer-Cripps, J. Mater. Sci. 32 (1997) 5653-5659.
[5] A.C. Fischer-Cripps, J. Mater. Sci. 34 (1999) 129-137.
[6] E.R. Kral, K. Komvopoulos , D.B. Bogy, Trans. ASME 62 (1995) 20-28.
[7] L. Kogut, I. Etsion, ASME J. Appl. Mech. 69 (2002) 657-662.

[8] Y.J. Park, G.M. Pharr, Thin Solid Films 447-448 (2004) 246-250.
[9] B. Taljat, G.M. Pharr, Int. J. Solids Struct. 41 (2004) 3891-3904.
[10] M. Mata, O. Casals, J. Alcalá, Int. J. Solids Struct. 43 (2006) 5994-6013.
[11] X. Hernot, O. Bartier, Y. Bekouche, R. El Abdi, G. Mauvoisin, Int. J. Solids Struct. 43 (2006) 4136-4153.
[12] J. D. Bressan, A. Tramontin, C. Rosa, Wear 258 (2005) 115-122.
[13] N. Schwarzer, ASME J. Trib. 122 (2000) 672-681.
[14] H. Hertz, Aus den Verhandlungen des Vereins zur Förderung des Gewerbefleißes, Berlin, 1882, pp. 174-196.
[15] N. Schwarzer, J. Phys. D: Appl. Phys., 37 (2004) 2761-2772.
[16] N. Schwarzer, G. M. Pharr, Thin Solid Films 469-470 (2004) 194-200.
[17] FILMDOCTOR: free software demonstration package for modelling indentation, available in the internet at http://www.siomec.de.
[18] N. Yu, A.A. Polycarpou, T.F. Conry, Thin Solid Films 450 (2004) 295-303.
[19] N. Schwarzer: "The extended Hertzian theory and its uses in analysing indentation experiments", Phil. Mag. 86(33-35) 21 Nov - 11 Dec 2006 5153 – 5767, Special Issue: “Instrumented Indentation Testing in Materials Research and Development”
[20] N. Schwarzer, I. Hermann, T. Chudoba, F. Richter: ”Contact Modelling in the Vicinity of an Edge”, Surface and Coatings Technology 146-147 (2001) 371-377
[21] Ilja Herrmann, PhD thesis, Chemnitz University of Technology, 2004, available in the internet at http://archiv.tu-chemnitz.de/pub/2004/0167